HIGH FRAME RATE COMPOUNDING FOR NONLINEAR B/A PARAMETER ULTRASOUND IMAGING IN ECHO MODE - SIMULATION RESULTS

Matthieu Toulemonde [a,b], François Varray [a], Olivier Basset [a], Piero Tortoli [b], Christian Cachard [a]

[a] CREATIS, Université de Lyon, INSA-Lyon, Université Lyon 1, CNRS UMR 5220, Inserm U630, Villeurbanne, France

[b] Microelectronics Systems Design Laboratory, Università di Firenze, Italy

ABSTRACT

The nonlinearity *B/A* parameter is an important parameter influencing the distortion of ultrasound waves in tissue. *B/A* has different values for normal and pathological media and can be used for tissue characterization. The extended comparative method (ECM) allows estimating the *B/A* parameter in echo mode configuration but presents some limitations. The limitations are the concentration of energy due to transmission focusing and the poor resolution in distinguishing areas with different *B/A*. This paper proposes to improve the estimation of *B/A* with the ECM approach using a high frame rate imaging approach based on plane wave transmission. The simulation results show that good performance in *B/A* estimation can be obtained through the analysis of the corresponding pressure field. Promising results are also achieved through the direct estimation of *B/A* from the B-Mode echo-mode images.

Index Terms— Ultrasound, High Frame Rate imaging, nonlinear propagation, nonlinearity parameter

1. INTRODUCTION

Nowadays, ultrasound imaging is a common diagnostic tool thanks to its non-invasive behavior and relatively cheap equipment. During the propagation of an ultrasound wave, harmonic frequencies are generated by the nonlinear properties of the tissue. The quantification of the nonlinearity is based on the evaluation of the nonlinear tissue *B/A* parameter which strongly influences the harmonics generation. The *B/A* parameter has different values in normal and pathological tissues and its measurement may have high diagnostic value [1-3]. Several methods are used to estimate the *B/A* parameter and can be grouped in two main families: thermodynamic and finite amplitude methods [4]. Thermodynamic methods have a good accuracy but need specific equipment to perform the measurement, while the finite amplitude methods can be used in echo mode and are thus suitable for clinical applications.

All these approaches can use different techniques [1-7] to calculate the *B/A* parameter. In particular, a recent study has proposed an extended comparative method (ECM) to image the *B/A* parameter in inhomogeneous nonlinear media [5]. However, this technique presents drawbacks. First, the focalization used during the transmission concentrates the energy at one particular depth which is then not homogeneous on the image. Second is the inaccurate delimitation of areas with different *B/A* in the media. Finally, the accuracy is limited by the presence of speckles in the image.

In this paper we propose the combination of the ECM method with high frame rate (HFR) compounding [8]. The HFR compounding technique is based on the transmission of multiple steered plane waves and post processing reconstruction. Plane waves are not focused and the combination of multiple plane waves steered at different angles allows to cover a sector angle and to decrease the speckle. In the method implemented here, the speckle reduction is completed by processing the images with the alternative sequential filter (ASF).

The paper is organized as follows. The first part includes a brief review of the nonlinear propagation theory and of the nonlinear *B/A* estimation with ECM approach. Then, the HFR compounding approach is described. Next, we propose an approach to estimate the *B/A* parameter from the pressure field and from the B-mode image. In the latter case the pressure field is not available and we assume that it is directly related to the B-mode image amplitude.

2. EXTENDED COMPARATIVE METHOD

The *B/A* parameter can be related to the Taylor series expansion of the pressure wave $p = p(\rho, s)$ in a medium with constant entropy $s = s_0$ [6]:

$$p - p_0 = \left(\frac{\partial p}{\partial \rho}\right)_{0,s} (\rho - \rho_0) + \left(\frac{\partial^2 p}{\partial \rho^2}\right)_{0,s} \frac{(\rho - \rho_0)^2}{2} + \cdots \qquad (1)$$

where ρ is the density of the medium, p_0 and ρ_0 are the pressure and density values at equilibrium. Equation (1) is simplified using $P = p - p_0$ and $\rho' = \rho - \rho_0$:

978-1-4799-2893-4/14/$31.00 ©2014 IEEE

$$P = A\frac{\rho'}{\rho_0} + \frac{B}{2!}\left(\frac{\rho'}{\rho_0}\right)^2 + \cdots \quad (2)$$

$$A = \rho_0\left(\frac{\partial P}{\partial \rho}\right) \equiv \rho_0 c_0^2 \quad (3)$$

$$B = \rho_0^2\left(\frac{\partial^2 P}{\partial \rho^2}\right) \quad (4)$$

The *B/A* ratio can be expressed as a function of the sound velocity c_0 and the density of the medium from (3) and (4):

$$\frac{B}{A} = \frac{\rho_0}{c_0^2}\left(\frac{\partial^2 P}{\partial \rho^2}\right) \quad (5)$$

In the literature, the nonlinearity coefficient β, which is related to *B/A*, is also used:

$$\beta = 1 + B/2A \quad (6)$$

The extended comparative method (ECM) finds its origin in the insertion-substitution method developed in [5;7]. The objective is to compare a reference medium with known nonlinearity coefficient β_0 to another one with unknown nonlinearity coefficient β_i. ECM is based on the evaluation of the amplitude pressure of the second-harmonic wave, p_2, which is expressed as [7]:

$$p_2(z) = \frac{\pi f p_0^2}{\rho_0 c_0^3}\int_0^z \beta(u)\exp\left(\int_0^u -2\alpha_1(v)dv - \int_u^z \alpha_2(v)dv\right)du \quad (7)$$

where α_1 and α_2 are the attenuation coefficients of fundamental and second-harmonic waves of the medium, respectively.

In the case of homogeneous nonlinearity coefficient and attenuation in the reference medium, equation (7) could be expressed as [5]:

$$p_{20}(z) = \frac{\beta_0 \pi f p_0^2}{\rho_0 c_0^3} I_0(z) \quad (8)$$

where

$$I_0(z) = \frac{e^{-2\alpha_{10}z} - e^{-\alpha_{20}z}}{\alpha_{20} - 2\alpha_{10}} \quad (9)$$

Based on the comparative method, the ratio between the pressure amplitude of the second harmonics in the unknown medium, subscript *i*, and the reference medium, subscript 0, gives:

$$\frac{p_{2i}(z)}{p_{20}(z)} = \frac{\rho_0 c_0^3}{\rho_i c_i^3}\frac{e^{\int_0^u -\alpha_{2i}(v)dv}\int_0^z \beta_i(\mu)e^{\left(\int_0^z (\alpha_{2i}(v)-2\alpha_i(v))dv\right)}d\mu}{\beta_0 I_0(z)} \quad (10)$$

$$\frac{\beta_i(z)}{\beta_0} = \frac{\rho_i c_i^3}{\rho_0 c_0^3}\left[V(z)\frac{p_{2i}}{p_{20}} + W(z)\frac{d}{dz}\left(\frac{p_{2i}}{p_{20}}\right)\right] \quad (11)$$

where *V(z)* and *W(z)* are two terms depending on the attenuations of the two different media:

$$\begin{cases} V(z) = \dfrac{e^{-2\alpha_{10}z}(\alpha_{2i}(z) - 2\alpha_{10}) - e^{-\alpha_{20}z}(\alpha_i(z) - \alpha_{20})}{\alpha_{20} - 2\alpha_{10}} e^{\int_0^z 2\alpha_{1i}(v)dv} \\ W(z) = I_0(z)\,\mathrm{e}^{\int_0^z 2\alpha_i(v)dv)} \end{cases} \quad (12)$$

The final equation in (11) is valid in media with different densities, celerity and attenuations. If the attenuations are considered equal in the two media and homogenous during the propagation, *V* and *W* are simplified as:

$$\begin{cases} V(z) = 1 \\ W(z) = \dfrac{1 - e^{-(\alpha_1 - 2\alpha_2)z}}{\alpha_2 - 2\alpha_1} \end{cases} \quad (13)$$

which leads to a simplified expression of the nonlinearity coefficient:

$$\beta_i(z) = \beta_0(z)\frac{\left(\rho c^3\right)_i}{\left(\rho c^3\right)_0}\left[\frac{p_{2i}}{p_{20}} + \frac{1 - e^{-(\alpha_2 - 2\alpha_1)z}}{\alpha_2 - 2\alpha_1}\frac{d}{dz}\left(\frac{p_{2i}}{p_{20}}\right)\right] \quad (14)$$

The equation (14) shows that β_i depends on the ratio, p_{2i}/p_{20}, of the local pressures. This approach is thus feasible in simulation or when the pressure is directly measurable in the media with a hydrophone.

In echo-mode, the pressure field of the medium is unknown, since only RF images or B-mode images are acquired. B-mode images exhibit a speckle texture created by the scatterers in the medium. It is assumed in this paper that the local pressure can be derived from B-mode images local amplitude. However, ECM cannot be directly applied on B-mode images because the speckle has a deleterious effect on the derivative term in (14) [5]. To limit the speckle noise, the alternative sequential filter (ASF) can be used. ASF is based on mathematical morphology operations [9]. It consists in the composition of several opening and closing operations on B-mode images with masks of increasing sizes.

It is also supposed that the intensity variation on fundamental images depends on some factors related to the scatterers' distribution. In addition, in second-harmonic images, the intensity variation depends also on the nonlinearity parameter while fundamental images depend only on the scatterer's distribution. So the normalization, pixel by pixel, of the second harmonic image by the fundamental image suppresses the intensity variation coming from the scatterer's distribution and only the nonlinearity parameter intensity variation remains.

In summary, the first step to estimate *B/A* consists in applying a 5th order Butterworth filter on the RF simulated data to separate the fundamental and second harmonic RF images, followed by an envelope detection to obtain B-mode images. Then, the ASF technique is applied on both B-mode images. Next, the second-harmonic image is normalized by the fundamental image. The resulting image is the input of the ECM method.

3. HIGH FRAME RATE COMPOUDING TECHNIQUE

In HFR imaging, a plane wave is transmitted over a wide probe aperture. Through an offline processing,

backscattered echoes from the insonified region can be recombined to form one RF image [8, 10]. A single illumination doesn't produce a good B-mode image quality. Montaldo *et al.* thus proposed HFR compounding to improve the image quality [8]. Multiple steered plane waves, covering a sector angle, are consecutively transmitted. Different lines of the RF image, obtained for each illumination, are calculated using the echoes backscattered to the same transducer elements applying specific sets of time delays. The final compounded image is a coherent average of the RF images obtained from all illuminations. The use of different steering angles increases the quality of the B-mode images in terms of resolution, contrast and noise and artifacts reduction, while increasing the acquisition time.

4. SIMULATIONS

For nonlinear propagation, the CREANUIS simulator has been used [12]: it simulates the fundamental and second-harmonic pressure fields coupled with the RF images.

The nonlinearity *B/A* parameter estimation, based on the combination of ECM with HFR, has been obtained using (14) in two types of simulation. In the first case, *B/A* has been directly estimated from the pressure field, while in the second one, the estimation is based on echo-mode simulated images.

For both simulations, two nonlinear media have been considered. One is composed of a background with *B/A*=5 and an elliptic inclusion with *B*/A=10. The second medium is similar, except that inside the elliptic inclusion, two regions with different nonlinearity parameters (3 and 7) were included. Schematic representations of the nonlinearity *B/A* parameter are given in Figure 1.a and Figure 1.e. The two vertical lines in each figure indicate the medium used as a reference in the ECM. The nonlinearity parameter is homogeneous inside this region. Each simulated phantom includes 700 000 scatterers (11.16 scatterers / mm^3) randomly distributed in space and amplitude.

A 4-cycle sinusoidal burst at 3 MHz weighted by a Gaussian window was transmitted from each element. No spatial apodization was used in both transmission and reception. The probe parameters are given in the Table 1.

Parameters	Value
Number of elements	256
Number of active elements	64
Pitch	245 µm
Kerf	30 µm
Height	6 mm
Elevation focus	23 mm

Table 1: Summary of the probe parameters

Two different transmission strategies were used in HFR imaging: single plane wave transmission and compounding, with one illumination at 0° and seven illuminations from -1.5° to 1.5° with 0.5° angle step.

For plane wave transmission, the 256 probe elements are simultaneously fired to explore the entire nonlinear medium. If steering is used, the second-harmonic pressure field image is the average of second-harmonic pressure field obtained for each angle.

For comparison, a standard B-Mode image with single transmission focused at 60 mm was also simulated. In this case, 64x256 transmissions were done. Each emission with 64 elements allows to produce one line of the second harmonic field image.

4.1. Pressure field *B/A* estimation

The objective of this experiment was to estimate the *B/A* parameter with the pressure field approach. In this case, (14) was directly applied.

The estimated *B/A* images for both nonlinearity media are given in Figure 1. The mean value and the standard deviation of the *B/A* parameter in each area are given in Table 2 and Table 3. Figure 1 shows that the use of HFR with 7 angles improves the *B/A* area delimitation compared to SF approach. HFR with one angle is not suitable to correctly determine the *B/A* area.

4.2. B-mode *B/A* estimation

The objective of this experiment was to estimate the *B/A* parameter from B-mode images. The pressure field approximation explained in section 2 is applied here.

The estimated *B/A* images for both nonlinearity media are given in Figure 2. The mean value and the standard deviation of the *B/A* parameter in each area are given in Table 4 and Table 5. From Figure 2, the use of HFR approach with seven angles improves the *B/A* area delimitation compared to SF approach in the simple nonlinear media. In the complex media the improvement is less significant because the speckle noise is not successfully suppressed.

5. CONCLUSION AND DISCUSSION

In this paper we have proposed to use HFR compounding to improve the *B/A* estimation. Using plane wave transmission, no depth is "privileged", contrarily to focused transmission approaches. The simulations made with SF for different focal depth, 30 mm 60 mm and 100 mm, show that the *B/A* estimation is not satisfying when the target is outside the focal point.

In pressure field simulations, *B/A* with 7-angle HFR and with SF was estimated. Varray et al. report that the ECM approach has difficulties to estimate variations in the nonlinearity parameter [5]. The SF method is actually more sensitive to this problem than 7-angle HFR because the HFR approach uses different views of the same media.

The delimitation of *B/A* areas is better in 7-angle HFR approach than in SF method.

In B-mode images, Figures 2 and Tables 4 and 5 show the feasibility of the *B/A* estimation based on the hypothesis that the B-Mode image is correlated to the pressure field. In the simple nonlinear medium, the *B/A* estimated for SF and 7-angle HFR are close to each other. For the complex medium the estimation is more difficult. This problem comes from the hypothesis which considers that the pressure field is directly related to the intensity in the B-mode image. The speckle pattern, remaining after filtering, hampers the correct estimation by ECM. A new approach using multitaper has been presented to smooth speckle [13]. This approach has already been combined with HFR compounding and will be tested to improve the *B/A* estimation.

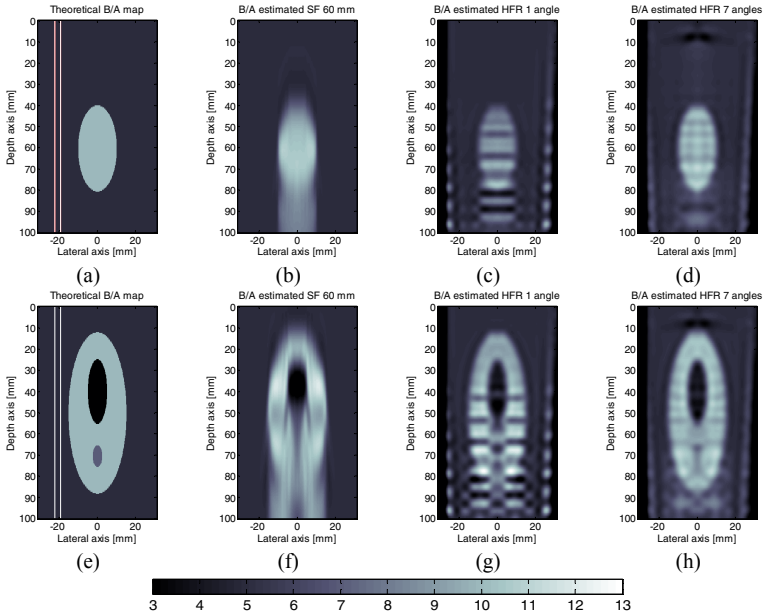

Figure 1: CREANUIS *B/A* estimation with second-harmonic pressure field for SF and HFR approaches for two different *B/A* media.

B/A	SF 60 mm		HFR 1		HFR 7	
	Mean	STD	Mean	STD	Mean	STD
5	**5.28**	0.84	**4.54**	1.81	**4.58**	1.86
10	**9.74**	0.91	**7.9**	1.01	**9.47**	0.82

Table 2: Nonlinearity *B/A* parameter estimated with simulated pressure field for a simple nonlinear B/A medium.

B/A	SF 60 mm		HFR 1		HFR 7	
	Mean	STD	Mean	STD	Mean	STD
3	**4.31**	1.82	**4.92**	1.16	**4.89**	1.11
5	**5.5**	1.14	**4.52**	2.17	**4.54**	2.13
7	**8.43**	0.45	**7.3**	1.24	**8.45**	0.61
10	**9.64**	1.07	**8.89**	1.4	**9.54**	0.84

Table 3: Nonlinearity *B/A* parameter estimated with simulated pressure field for a complicated nonlinear *B/A* medium.

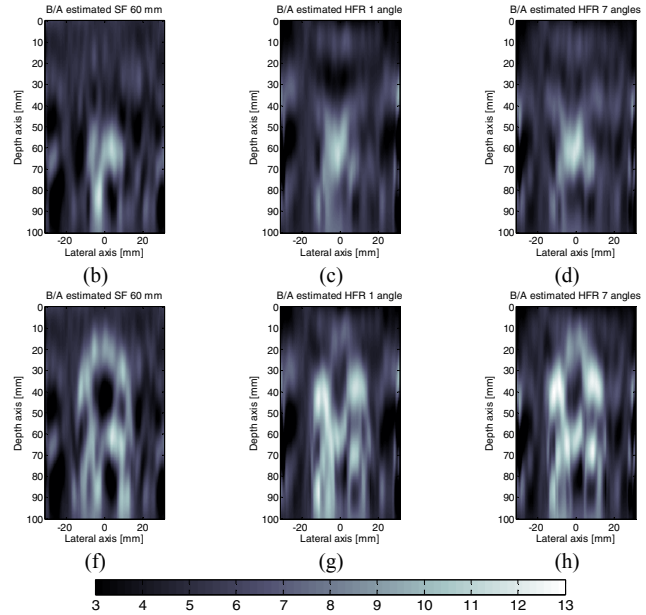

Figure 2: CREANUIS *B/A* estimation with B-mode images for SF and HFR approaches for two different *B/A* media.

B/A	SF 60 mm		HFR 1		HFR 7	
	Mean	STD	Mean	STD	Mean	STD
5	**4.99**	1.25	**5.18**	1.11	**5.1**	0.94
10	**7.76**	1.67	**7.97**	1.40	**8.01**	1.77

Table 4: Nonlinearity *B/A* parameter estimated with simulated pressure field for a simple nonlinear *B/A* medium.

B/A	SF 60 mm		HFR 1		HFR 7	
	Mean	STD	Mean	STD	Mean	STD
3	**4.27**	1.80	**6.61**	1.52	**6.45**	1.41
5	**5.2**	1.55	**5.22**	1.80	**5.19**	1.54
7	**6.59**	1.26	**7.62**	1.54	**8.02**	1.86
10	**7.82**	1.83	**8.39**	1.90	**8.8**	2.08

Table 5: Nonlinearity *B/A* parameter estimated with simulated pressure field for a complicated nonlinear *B/A* medium.

Special thanks are due to ANR-11 TecSan-008-01 BBMUT and Centre Lyonnais dAcoustique (CeLya) – ANR-10-LABX-0060. This work was partially supported by the Italian Ministry of Education, Universities and Research (PRIN 2010-2011). The main author is financially supported by the Franco-Italian University with a VINCI grant and by the Rhône-Alpes region with an Explora'Doc grant.

6. REFERENCES

[1] X.Gong, Z. Zhu, T. Shi, J. Huang, "Determination of the acoustic nonlinearity parameter in biological media using FAIS and ITD methods", J. Acoust. Soc. Am., vol. 86, no. 1, pp. 1-5, 1989.

[2] W. K. Law, L.A Frizzell, F. Dunn, "Determination of the nonlinearity parameter B/A of biological media", *Ultrasound in Med. & Biol.*, vol. 11, no. 2, pp. 307-318, 1985

[3] X.Gong, D. Zhang, J. Liu, H. Wang, Y. Yan, X. Xu, "Study of acoustic nonlinearity parameter imaging methods in reflection mode for biological tissues", *J. Acoust. Soc. Am.*, vol. 116, no. 3, pp. 1819-1825, 2004.

[4] W.K. Law, L.A. Frizzell, F. Dunn, "Comparison of thermodynamic and finite amplitude methods of B/A measurement in biological materials", *J. Acoust. Soc. Am.*, vol. 74, no. 4, pp. 1295-1297, 1983.

[5] F. Varray, O. Basset, P. Tortoli, C. Cachard, "Extensions of Nonlinear B/A Parameter Imaging Methods for Echo Mode", *IEEE Trans. UFFC*, vol. 58, no. 6,pp. 1232-1244, 2011.

[6] R.T. Beyeyr, "Parameter of Nonlinearity in Fluids", *J. Acoust. Soc. Am.*, vol 32, no. 6, pp. 719-721, 1960.

[7] D. Zhang, X. Gong, S. Ye, "Acoustic nonlinearity parameter tomography for biological specimens via measurements of the second harmonics", *J. Acoust. Soc. Am.*, vol. 99, no. 4, pp. 2397-2402, 1996.

[8] G. Montaldo, M. Tanter, J. Bercoff N/ Benech, and M. Fink, "Coherent plane-wave compounding for very high frame rate ultrasonography and transient elastography". in *IEEE UFFC*. vol. 56. no. 3. pp. 489-506. 2009.

[9] S.R. Sternberg, "Grayscale Morphology", in *Computer Vision, Graphics, and Image Processing*, vol. 35, no. 3, pp. 33-355, 1986.

[10] J. Cheng, J-yu. Lu, "Extended high-frame rate imaging method with limited-diffraction beams", in *IEEE UFFC*, vol. 53, no. 5, pp. 880-899, 2006.

[11] J-yu. Lu, "2D and 3D high frame rate imaging with limited diffraction beams". in *IEEE UFFC*, vol. 44, no. 4, pp. 839-856, 1997.

[12] F. Varray, O. Basset, P. Tortoli, and C. Cachard, "CREANUIS: A Nonlinear Radio Frequency Ultrasound Image Simulator", in *Ultrasound in Medicine and Biology*, vol. 39, no. 10, pp. 1915-1924, 2013.

[13] A.C. Jensen. S.P. Näsholm. C.I.C. Nilsen. A. Austeng. S. Holm. "Applying Thomson's multitaper approach to reduce speckle in medical ultrasound imaging". in *IEEE UFFC*. vol. 59, no. 10. pp. 2178-2185. 2012.